Elucidating the Magma Plumbing System of the Active Volcano Ol Doinyo Lengai, Natron Rift, Tanzania Using Geodesy and Numerical Modeling

N. Daud, D. S. Stamps, M. Battaglia, M.H. Huang, E. Saria, K.H. Ji, K. Popolizio
dntambila@vt.edu, dstamps@vt.edu, mbattaglia@usgs.gov, mhhuang@umd.edu, saria.elifuraha@gmail.com, khji@kigam.re.kr, kelspop@vt.edu
Virginia Tech, USA -- USGS and the University of Rome, Italy -- University of Maryland, College park, USA -- Ardhi University, Tanzania -- Korea Institute for Geosciences and Mineral Resources

1.0 INTRODUCTION

Volcanic deformation evolves through a series of distinct stages during continental rifting and is a key element in causing geohazards. Volcanic eruptions are governed by the magmatic plumbing system of the volcano which sets the stage, style, occurrences and the magnitude of eruptive activity. An understanding of magma plumbing systems is vital for effective volcanic monitoring and hazard mitigation.

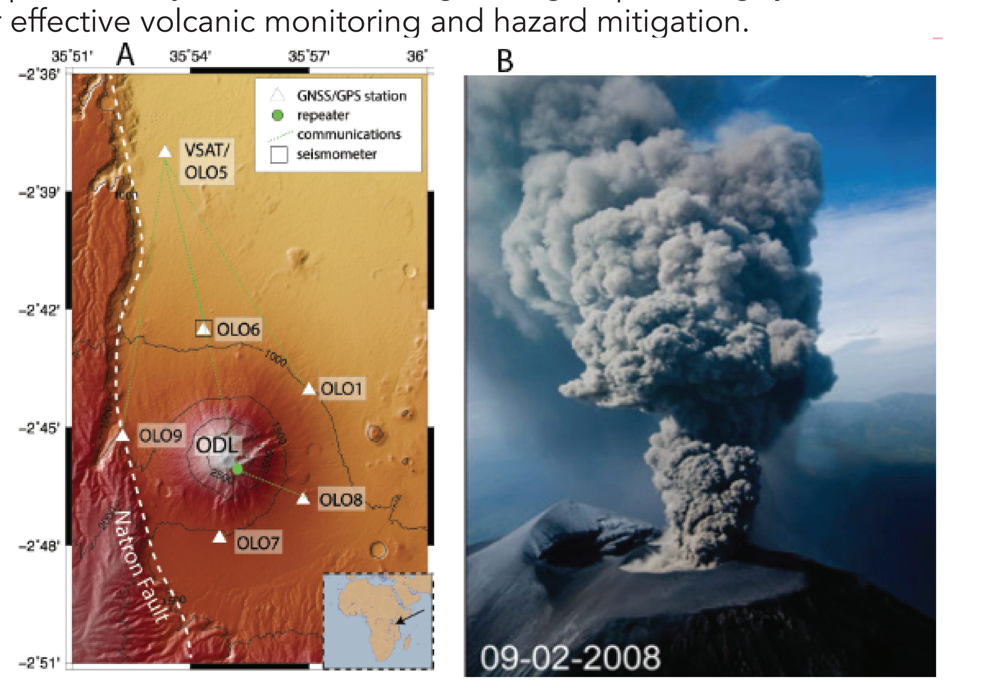

Figure 1A. The TZVOLCANO permanent GNSS network. B. Ol Doinyo Lengai volcanic eruption during the 2007-2008 explosive episode (from Kervyn et al., 2010).

Ol Doinyo Lengai (ODL) is the only active volcano worldwide known to erupt low-temperature carbonatites. Between 2007 and 2010, the volcano has had several explosions, and it erupted with ash falls and lava flows (VEI 3) (Figure 1B) that caused damage to the nearby communities. Its volcanic system in part is poorly understood due to lack of precise surface deformation measurements.
The aim of this work is to investigate the magmatic system of ODL using geodesy and numerical modeling to better understand the subsurface plumbing system.

2.0 TECTONIC SETTING

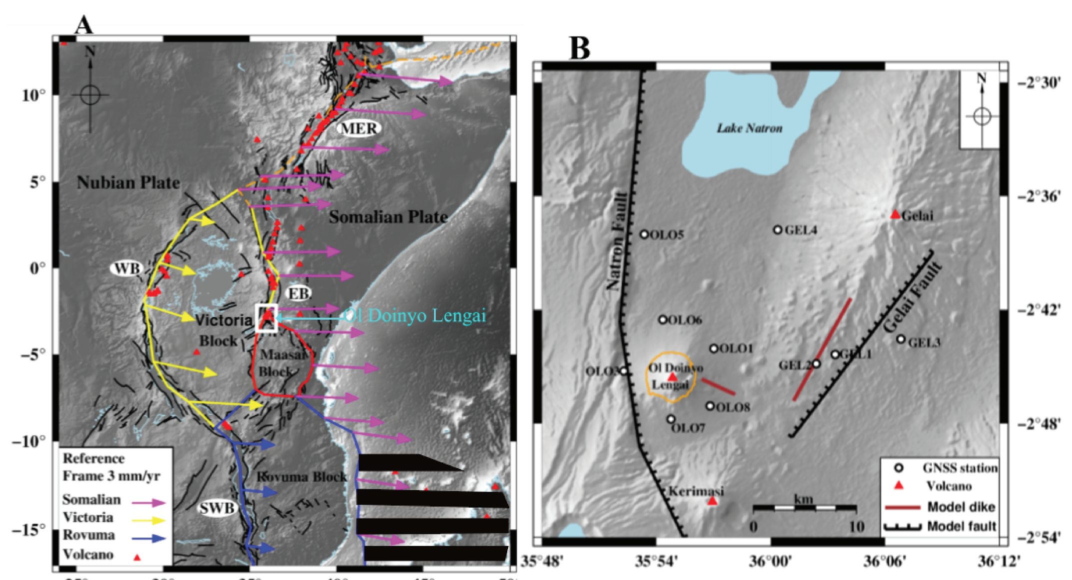

Figure 2A. The continental East Africa Rift. B. A simplified section of the Natron Rift. Faults are black lines with tick marks. The active Ol Doinyo Lengai, the two dormant volcanoes, Gelai and Kerimasi (triangle in red), continuous GNSS stations (OLO1-OLO8) constituting the permanent TZVOLCANO network (white circles) and GEL1-GEL4 are campaign sites

Ol Doinyo Lengai is a polygenetic stratovolcano within the Natron Rift, along the southern Eastern Branch of the East African Rift System (Figure 1A) characterized by the presence of the Natron rift adjacent to the Victoria microplate and the Gelai fault to the east (Figure 1A, B). The Natron rift extends eastward at ~3.8 mm/yr relative to the Nubian Plate (Stamps et al., 2021).

2.1 Hypothesis

We hypothesis that the onset, size, duration and hazard of eruptions are influenced by the volcanic system. To address the hypothesis, we investigate the magma plumbing system of ODL using the inverse USGS code dMODELS (Battaglia et al., 2013) to solve for different magma sources embedded in a homogeneous and elastic half space. We invert both GNSS data and InSAR data with dMODELS.

3.0 METHODS

3.1 Global Navigation Satellite System (GNSS)

We use five years of data (2016 – 2021) from the TZVOLCANO network (Figure 1A). We process GNSS observations using GAMIT-GLOBK software (Herring et al., 2018). The time-series (Figure 3) from TZVOLCANO were processed to examine and monitor the impending eruptive activity of the volcano.

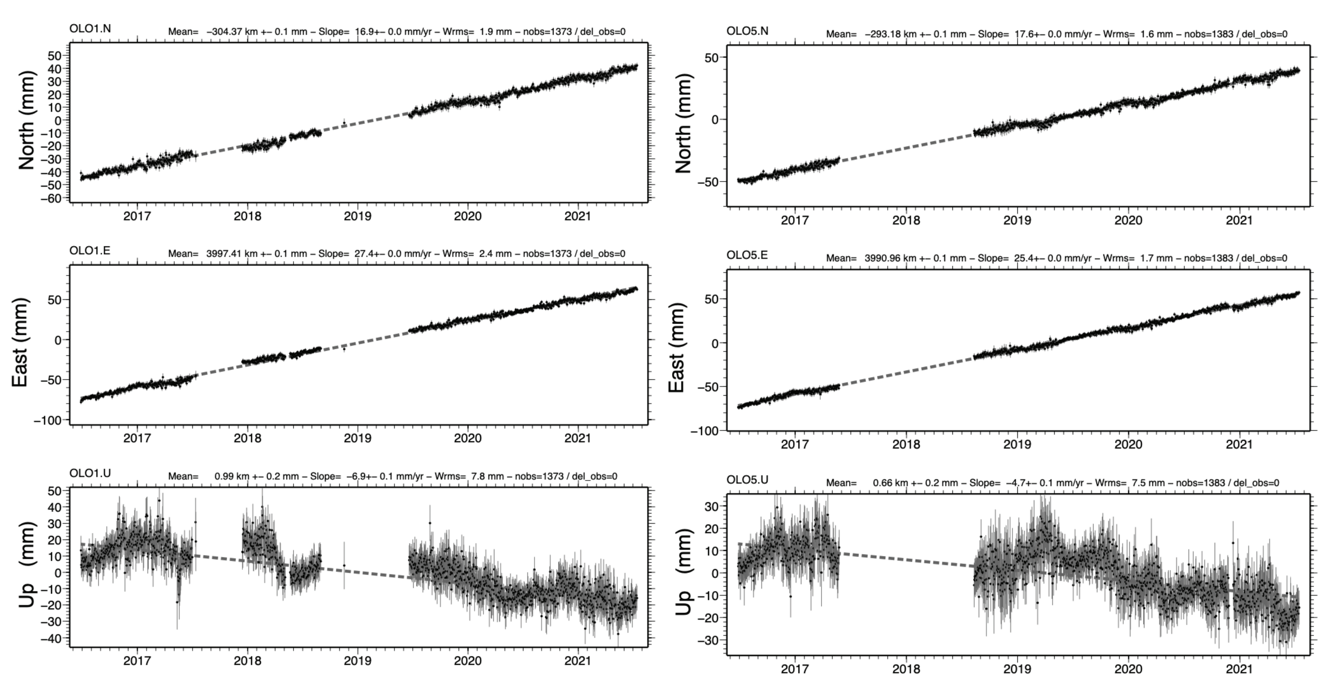

Figure 3. Time series for OLO1 and OLO5 GNSS stations

We evaluate the noise characteristics of the velocity solution using the real sigma algorithm to account for time-correlated noise present in GLOBK algorithms (Reilinger et al., 2006; Saria et al., 2013). In addition we accounted for annual and semi-annual signals that are likely to affect the solutions using the code HECTOR (Bos et al., 2013). The resulting velocity field (Figure 6A,B) is used in the inversion of ground deformation around the Ol Doinyo Lengai.

3.2 Interferometric Synthetic Aperture Radar (InSAR)

We use five years (2016-2021) of the Copernicus Sentinel-1 Synthetic Aperture Radar (SAR) C-band (wavelength ~56 mm) data to generate Interferometric Synthetic Aperture Radar images in order to measure surface motions. We process the data using the Scientific Computing Environment (ISCE) TOPS stack processor (Rosen et al., 2012; Fattahi et al., 2017) and the Miami INsar Time-series software (MintPy; Yunjun et al., 2019) to generate the InSAR time series (Figure 4).

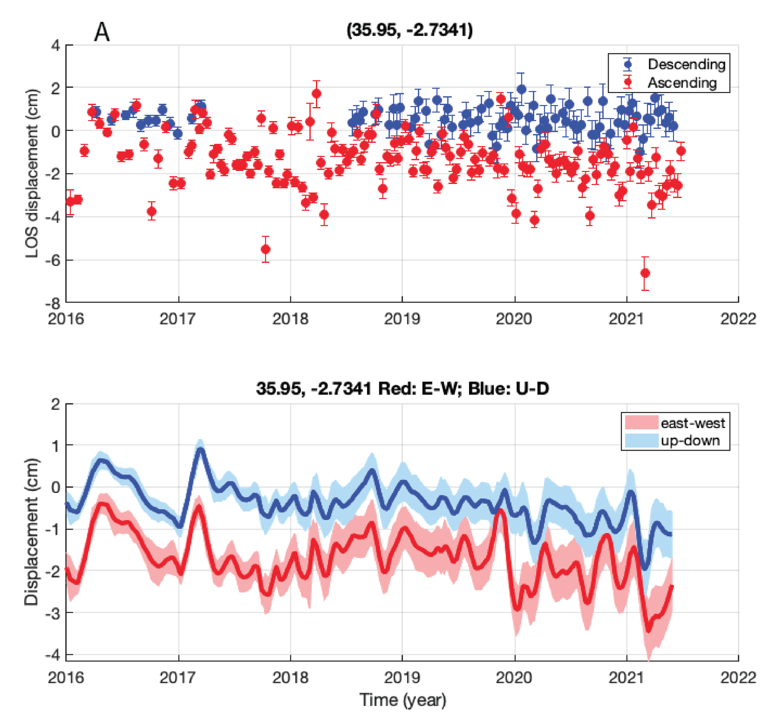

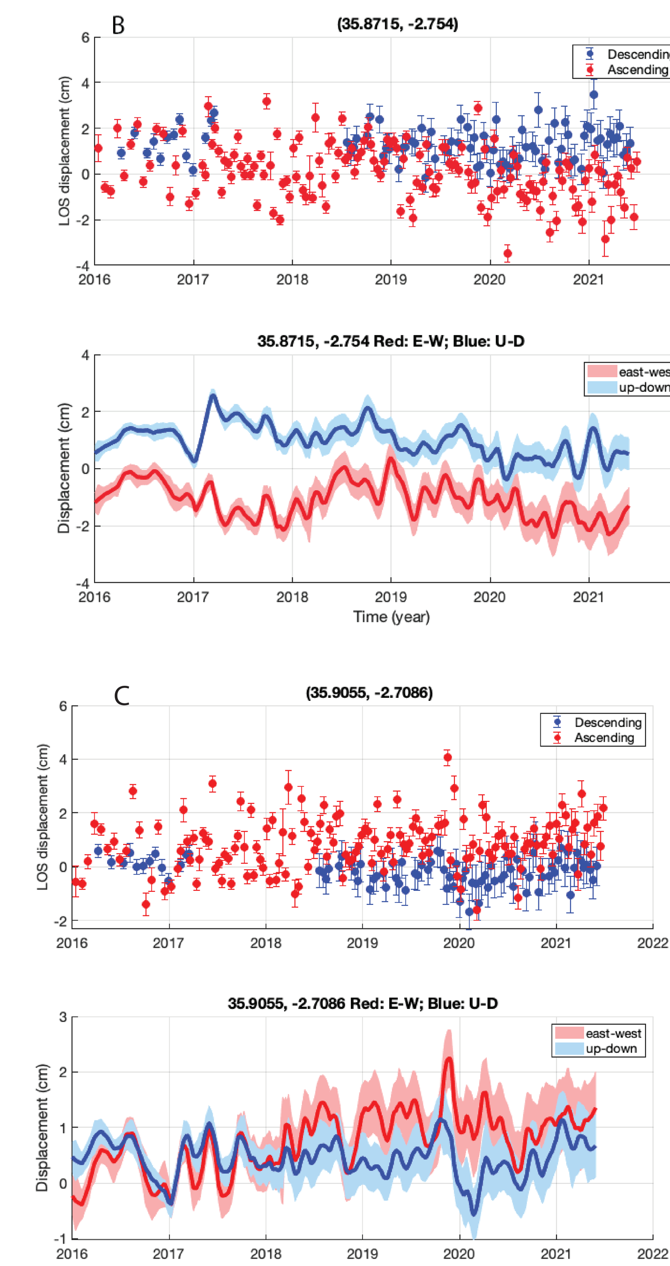

Figure 4A, B and C InSAR time series for OLO1, OLO3 and OLO6 respectively

3.3 Numerical Modeling with dMODELS

We employ the dMODELS program (Battaglia et al., 2013) to invert GNSS and InSAR observations to determine the geometry and parameters of the volcanic source. The software is based on a weighted least-squares inversion algorithm combined with a random search grid to determine the best-fit parameters for the volcanic deformation source by searching the minimum penalty function. We calculate magma reservoirs that are spherical (McTigue, 1987), spheroidal (Yang et al., 1988), sill (Fialko et al., 2001), or for a closing dike source that is modeled as a dislocation (Okada, 1985).

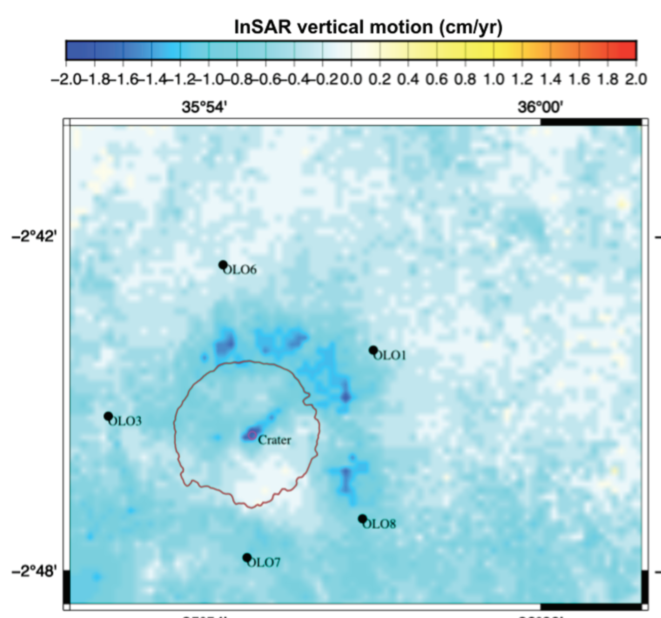

Figure 5. InSAR vertical velocity solution

4.0 RESULTS

4.1 GNSS velocity fields solution

We present horizontal and vertical velocity field solutions of the TZVOLCANO for the time frame of June 2016 to July 2021 (Figure 6A, B) at 2 sigma. The surface ground deformation was quantified using a local reference frame by fixing one single GNSS site, OLO5 in order to filter out the volcanic deformation from tectonic motion. We consider OLO5 to be stable and outside the influence of volcanic activity since it is located 19 north of the volcanic crater.

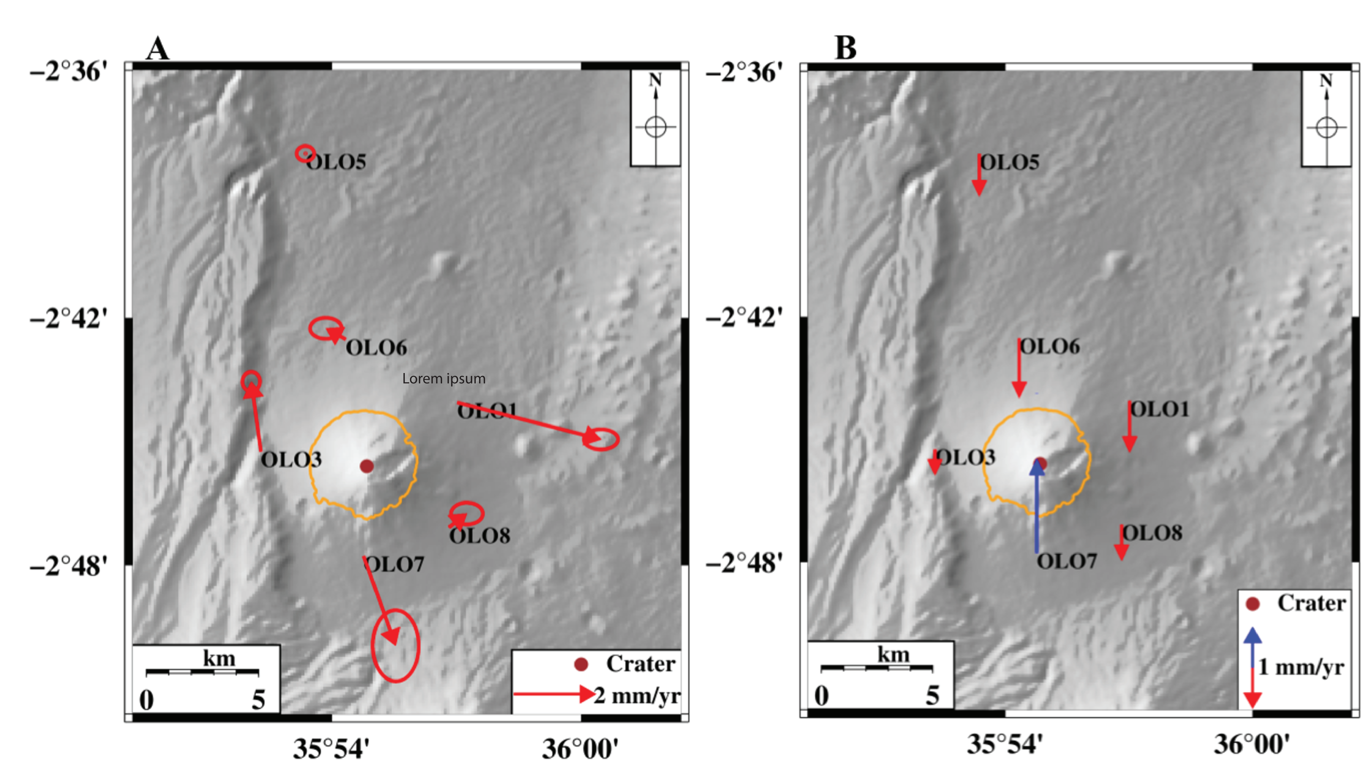

Figure 6A. TZVOLCANO horizontal velocity field solutions with respect to a fixed OLO5. B. Vertical velocity field solutions w.r.t ITRF14, contour (line filled orange) is the outline of Ol Doinyo Lengai.

4.2 InSAR velocity fields solution

We use both ascending (track 130) and descending (track 152) to estimate the vertical velocity (figure 5) for five years from 2016 to July 2021.

4.3 Inverse Modeling of GNSS velocities with dMODELS

Table 1. GNSS modeling result parameters for the deformation source

Source	χ^2_v	X_0 UTM (m)	±σ (m)	Y_0 UTM (m)	±σ (m)	Depth (m)	±σ (m)	Radius (m)	ΔV ($10^6 m^3$)	ΔV ±σ
Spherical	5.5	828547	157	9697259	78	1303	122	250	-0.05	0.01
Spheroidal	8.4	828414	118	9697252	38	927	262	400	-0.03	0.02

We present the GNSS inversion modeling result parameters for the tested subsurface magma sources (Table 1) and the corresponding horizontal and vertical velocities for the spherical (Figure 7 and 8).

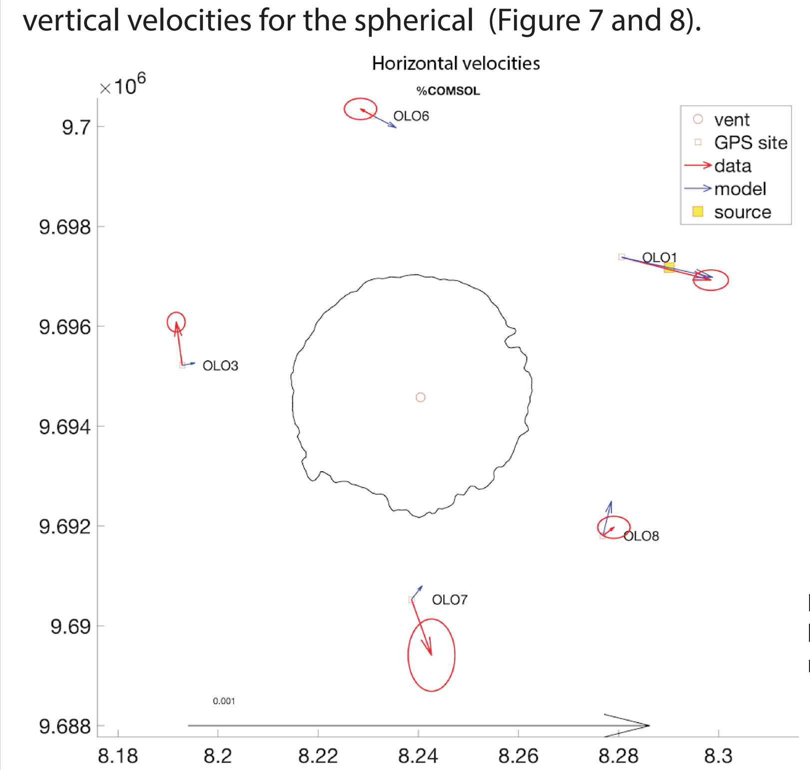

Figure 6. Horizontal velocity for the spherical model

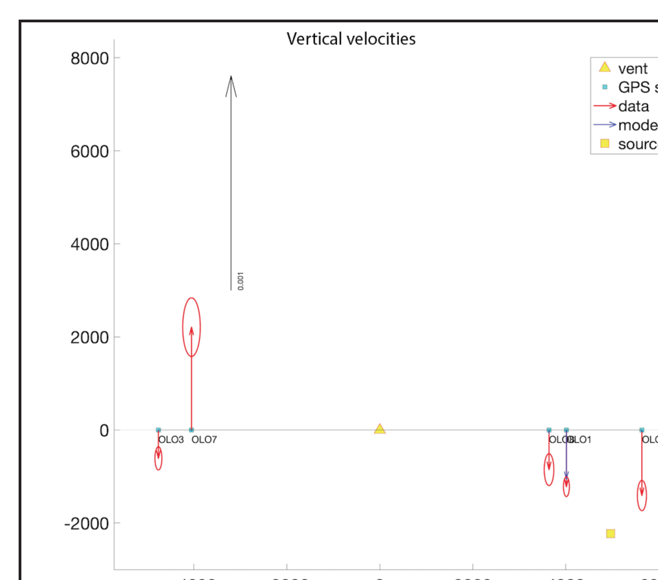

Figure 7. Vertical velocity for the spherical model

4.4 Inverse Modeling of InSAR velocities with dMODELS

We present a closing dike model near the Ol Doinyo Lengai (Figure 8, A-C) at a depth of ~9 km that best-fit InSAR inversion.

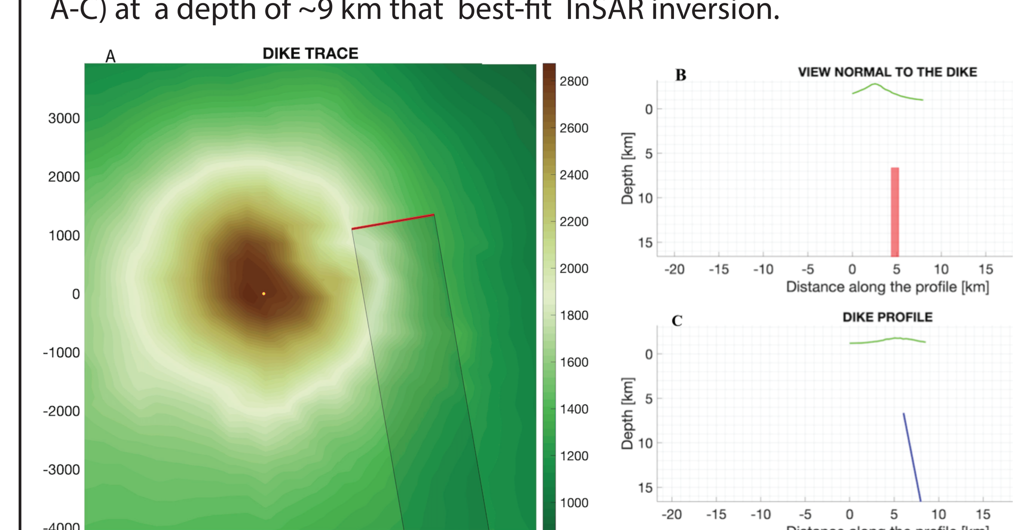

Figure 8A. Dike trace . B. View normal to the dike. C. Dike profile

5 RESULT DISCUSSION

Both GNSS and InSAR measurements are consistence depecting subsidence at a low rate (-1 to -2 mm/yr) although OLO7 is uplifting.

GNSS inversions suggest a shallow deflating volcanic source at ~1.3 km depth east of ODL (Figure 9).

InSAR alone quantifies a closing dike (~9 to 15 km depth, Figure 9) in a similar location to the resolved by Biggs et al. (2013).

The dike suggests a deep magmatic source at ~15 km (Baer et al., 2008; Calais et al., 2008; Biggs et al., 2013; Reiss et al., 2021).

Our conceptual model is shown in Figure 9.

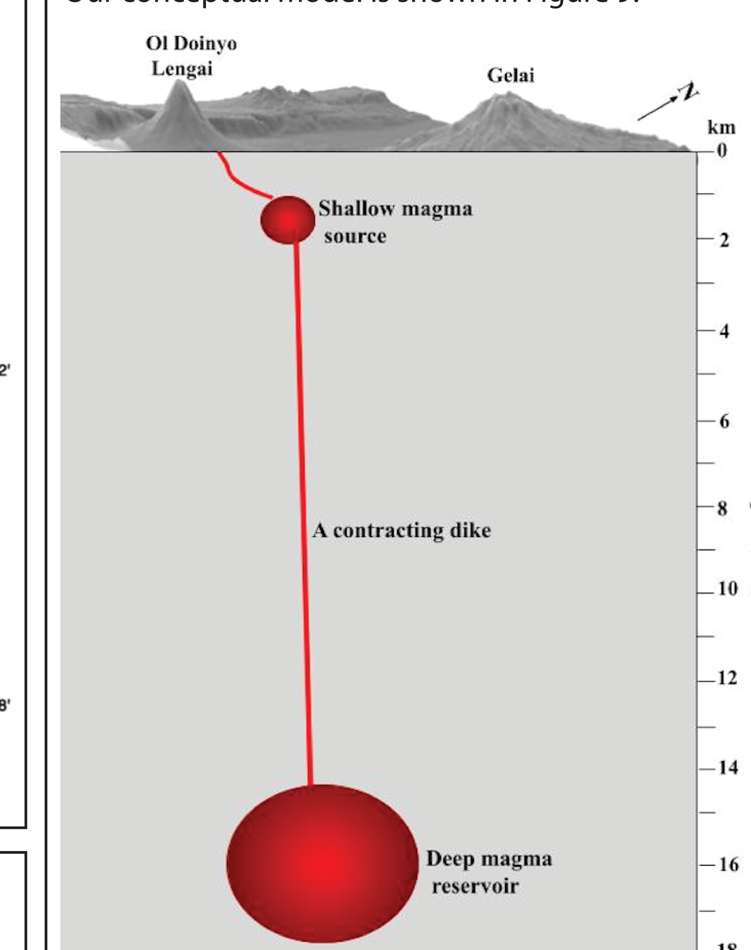

Figure 9. A conceptual model geometry of the magma plumbing system of Ol Doinyo Lengai between the shallow spherical source (~1.3 km), a contracting dike (~15 km) connecting a deep magma reservoir as quantified by GNSS and InSAR inversion from June 2016 to July 2021

6. CONCLUSION

This work suggests a shallow and deep magma reservoir exists east of ODL and that the 2007 dike is actively contracting.

The TZVOLCANO network quantifies the subsurface system, and can track volcanic signatures during volcanic unrest periods.

This work suggests an offset magmatic plumbing system feeds ODL.

7.REFERENCES

Battaglia, M., Cervelli, P. F., Murray, J. R., 2013. dMODELS: A MATLAB software package for modeling crustal deformation near active faults and volcanic centers. Journal of Volcanology and Geothermal Research, 254, 1-4. https://doi.org/10.1016/j.jvolgeores.2012.12.018

Biggs, J., Chivers, M., Hutchinson, M. C., 2013. Surface deformation and stress interactions during the 2007–2010 sequence of earthquake, dyke intrusion and eruption in northern Tanzania. Geophysics Journal of International. 195 (1), 16–26. https://doi:10.1093/gji/ggt226

Bos, M.S., Fernandes, R.M.S., Williams, S.D.P. and Bastos, L., 2013. Fast error analysis of continuous GNSS observations with missing data. Journal of Geodesy, 87(4), pp.351-360.https:/doi:10.1007/s00190-012-0605-0

Calais, E., d'Oreye, N., Albaric, J., Deschamps, A., Delvaux, D., Déverchère, J., Wauthier, C., 2008. Strain accommodation by slow slip and dyking in a youthful continental rift, East Africa. Nature 456 (7223), 783–787. https://doi:10.1038/nature07478

Fattahi, H., Agram, P., and Simons, M., 2017. A Network-Based Enhanced Spectral Diversity Approach for TOPS Time-Series Analysis. IEEE Transactions on Geoscience and Remote Sensing, 55(2), 777-786. doi:10.1109/tgrs.2016.2614925
Fialko, Y., Khazan, Y., Simons, M., 2001. Deformation due to a pressurized horizontal circular crack in an elastic half-space, with applications to volcano geodesy. Geophysical Journal International, 146(1), pp.181-190. https://doi.org/10.1046/j.1365-246X.2001.00452.x

Herring, T.A., King, R.W., Floyd, M.A. and McClusky, S.C., 2018. Introduction to GAMIT/GLOBK, Release 10.7: GAMIT/GLOBK Documentation.

Kervyn, M., Ernst, G. G. J., Keller, J., Vaughan, G., Klaudius, J., Pradal, E., Jacobs, P., 2010. Fundamental changes in the activity of the natrocarbonatite volcano Oldoinyo Lengai, Tanzania. II. Eruptive behavior. Bulletin of Volcanology. 72, 913–931. https://doi:10.1007/s00445-010-0360-0

McTigue, D.F., 1987. Elastic stress and deformation near a finite spherical magma body: resolution of the point source paradox. Journal of Geophysical Research: Solid Earth, 92(B12), pp.12931-12940. https://doi.org/10.1029/JB092iB12p12931

Reilinger, R., McClusky, S., Vernant, P., Lawrence, S., Ergintav, S., Cakmak, R., Ozener, H., Kadirov, F., Guliev, I., Stepanyan, R. and Nadariya, M., 2006. GPS constraints on continental deformation in the Africa-Arabia-Eurasia continental collision zone and implications for the dynamics of plate interactions. Journal of Geophysical Research: Solid Earth, 111(B5).https://doi.org/10.1029/2005JB004051

Reiss, M. C., Muirhead, J. D., Laizer, A. S., Link, F., Kazimoto, E. O., Ebinger, C. J., Rümpker, G., 2021. The impact of complex volcanic plumbing on the nature of seismicity in the developing magmatic natron rift, tanzania. front. Earth Sci, 8, 609805.

Rosen, P. A., Gurrola, E., Sacco, G. F., & Zebker, H. (2012). The InSAR scientific computing environment, Proc. EUSAR (pp. 730–733). Nuremberg, Germany.

Saria, E., Calais, E., Altamimi, Z., Willis, P., Farah, H., 2013. A new velocity field for Africa from combined GPS and DORIS space geodetic solutions: Contribution to the definition of the African reference frame (AFREF). Journal of Geophysical Research: Solid Earth, 118, 1677–1697. https://doi.org/10.1002/jgrb.50137.https://doi.org/10.1002/2013JB010901

Stamps, D.S., Kreemer, C., Fernandes, R., Rajaonarison, T.A. and Rambolamanana, G., 2021. Redefining East African Rift System kinematics. Geology, 49(2), pp.150-155.

Yang, X.M., Davis, P.M. and Dieterich, J.H., 1988. Deformation from inflation of a dipping finite prolate spheroid in an elastic half-space as a model for volcanic stressing. Journal of Geophysical Research: Solid Earth, 93(B5), pp.4249-4257.https://doi.org/10.1029/JB093iB05p04249
Yunjun, Z, Fattahi, H., and Amelung, F., 2019. Small baseline InSaR time series analysis: Unwrapping error correction and noise reduction,